

YU. PERLOVICH*, M. ISAENKOVA*, V. FESENKO*, H.J. BUNGE**

NEW-DISCOVERED REGULARITIES OF SUBSTRUCTURE INHOMOGENEITY AND DISTRIBUTION OF RESIDUAL MICROSTRESSES IN METAL MATERIALS WITH DEVELOPED DEFORMATION TEXTURE

NIEJEDNORODNOŚĆ SUBSTRUKTURY I ROZKŁAD MIKRONAPRĘŻEŃ WŁASNYCH W METALACH Z TEKSTURĄ DEFORMACJI

The substructure inhomogeneity of real textured metal materials was studied by use of the X-ray method of Generalized Pole Figures. Main regularities of substructure inhomogeneity were revealed for the first time. Substructure conditions of grains in rolled material form an extremely wide spectrum and vary by passing from texture maxima to texture minima, where residual deformation effects are most significant. The distribution of residual elastic microstrains in the orientational space of rolled material shows the distinct cross-wise system, consisting in alternation of quadrants with predominant microstrains of opposite signes.

Keywords: texture, X-ray line profile, generalized pole figure, crystallographic orientation, substructure inhomogeneity, residual microstrain.

Niejednorodność substrukтуры metali stekstutowanych badano za pomocą rentgenowskiej metody uogólnionych figur biegunowych. Ujawniono podstawowe prawidłowości niejednorodności substrukтуры. Substruktura ziaren materiału walcowanego tworzy ekstremalnie szeroki i zmieniający się obraz minimów i maksimów tekstury, w którym najważniejszymi są efekty deformacji własnej. Rozkład plastycznych mikrodeformacji własnych w przestrzeni orientacji materiału walcowanego wykazuje wyraźny układ naprzemiennych kwadrantów, w których dominują mikroodkształcenia przeciwnych znaków.

1. Introduction

The substructure inhomogeneity is a generally recognized feature of deformed metal materials. In this connection a question arises whether it is really possible to

* MOSCOV ENGINEERING PHYSICS INSTITUTE (STATE UNIVERSITY) MOSCOV, RUSSIA

** TU CLAUSTAHAL CLAUSTHAL-ZELLERFELD, GERMANY

discover some still unknown general regularities, controlling processes of structure development in metal materials. The positive answer to this question supposes a new methodical approach to the study of metals, based on the new paradigm of processes to be considered. This paradigm assumes that the substructure inhomogeneity is one of the most important properties of metal products, while the crystallographic orientation of grains (subgrains, blocks, cells etc.) is the best criterion for systematization of present inhomogeneities.

Numerous experiments on rolling of BCC single crystals had shown, that there are the stable orientations, characterized by sharply different strain hardening of single crystals and their tendency to recrystallization by the following annealing. In particular, single crystals of Mo in the stable orientation $\{001\}\langle 011 \rangle$ can be rolled up to very high deformation degrees by a low strain hardening and a decreased tendency to recrystallization, whereas similar single crystals in another stable orientation $\{111\}\langle 112 \rangle$ quickly strengthen and break already by small deformations [1]. These stable orientations correspond to main components in the final rolling texture of polycrystalline Mo, and it was natural to suppose that grains of these components differ in their strain hardening as the above rolled single crystals.

Since the plastic deformation usually is accompanied by arising of the crystallographic texture, development of the substructure inhomogeneity and the deformation texture prove to be mutually interconnected. When starting from concepts of texture formation, it can be anticipated that grains of the deformed polycrystal differ in substructure conditions, determined by initial and final orientations, active plastic deformation mechanisms, affiliation of the grain to that or another part of the texture maximum. But in order to make certain of this supposition by means of direct systematic measurements, an appropriate method had to be developed, enabling to obtain separately data on grains with any possible orientations. X-ray methods, due to their selectivity, allow to obtain separate data on grains with different orientations and presently give a single opportunity to study in details the complicated inhomogeneous substructure of textured materials. For this aim the diffractometric procedure was developed, combining texture measurements with analysis of the X-ray line profile.

Earlier similar X-ray procedures were used for the comparison of strain hardening, recovery and recrystallization in grains of main texture components as applied to rolled Mo-based alloys [1-4]. Obtained data agree with above-mentioned results of experiments on rolling of Mo single crystals: the energy of lattice distortion, accumulated in grains of the texture component $\{111\}\langle 112 \rangle$ proves to be much higher than in grains of the component $\{001\}\langle 011 \rangle$, and therefore the recovery in grains of the former component is accompanied by more significant changes of diffraction parameters than those in grains of the latter component, whereas their recrystallization temperature differ by 150-200°.

At present, when the automated X-ray equipment and the computer data treatment is accessible for most laboratories, methods for the systematic comparison of substructure conditions in all grains of textured metal material allow to give the fullest description of its inhomogeneous structure in terms of diffraction parameters and to

reveal new regularities, controlling the dependence of this inhomogeneity on the texture.

2. Experimental procedure and data treatment

The used experimental procedure consists in recording of the same X-ray line (hkl) by successive positions of the sample in the course of texture study (Fig.1), so that

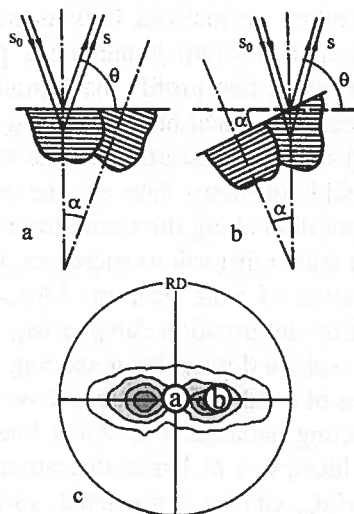


Fig. 1. geometry of the gpf method by the example of rolled Zr: the same X-ray line (0002), registered by positions (a) and (b), characterizes the condition of α -Zr crystalline lattice along basal axes with projections in the corresponding points of PF(0001) (c), distanced by angle α

the sample is characterized by the multitude of line profiles, corresponding to different orientations (ψ, φ) of reflecting planes $\{hkl\}$. X-ray line profiles can be registered by means of three different techniques: (1) 2θ — scanning by each successive position of the sample in the texture set; (2) the use of a position-sensitive detector (PSD); (3) the computational method, involving the treatment of several texture files, obtained by different positions 2θ of the usual detector. All X-ray measurements, referred in the given paper, were fulfilled using techniques (2) and (3) by SIEMENS texture diffractometers (D500/TX, D5000) and diffractometers of Russian manufacture (ДПОН-3, ДПОН-3М) with an automated texture set. Technique (2) gives the X-ray line profile as an immediate result of measurement with the PSD, whereas technique (3) reconstructs this profile on the basis of several fractions of its integral intensity for angular intervals ($2\theta_i \pm \Delta 2\theta$) under the supposition that it can be described by a function of certain type. In both cases we obtain finally parameters of approximating functions, though developed procedures of data treatment are different: the “fitting procedure”

as applied to profiles, directly measured with PSD, and the solution of equations set, corresponding to intensity measurements by different positions $2\theta_i$ of the usual detector.

The treatment of measured data includes correction for defocalization and absorption effects, approximation of X-ray line profiles with pseudo-Voigt functions, calculation of their parameters in view of results obtained for the annealed standard. This treatment is aimed to construction of so called Generalized Pole Figures (GPF), i.e. distributions of diffraction or substructure parameters in the stereographic projection of the sample [5-6].

Among diffraction parameters to be presented in GPF, along with integral intensity of X-ray line (the corresponding normalized GPF is the usual texture pole figure PF), there are its true physical half-width β and peak position 2θ , fraction of the Gauss function in the approximated line profile, background level, fitting error of the approximation procedure. Since a physical half-width β_{hkl} of X-ray line is determined by the size of coherent blocks and by distortion of the crystalline lattice along axes $\langle hkl \rangle$, the physical half-width of X-ray line can be considered as a generalized characteristic of the lattice condition along the normal to reflecting planes: as coherent domains become smaller and lattice distortions increases, the physical profile of X-ray line widens [7]. The distribution of peak position $2\theta(\psi, \varphi)$ can be recalculated into the distribution of lattice elastic deformation $\Delta d(\psi, \varphi)/d_{av}$ along crystallographic axes $\langle hkl \rangle$, where d_{av} — average weighted interplanar spacing and $\Delta d(\psi, \varphi) = d(\psi, \varphi) - d_{av}$ with signs “+” or “-” for cases of local elastic extension or contraction, respectively. By use of known models, connecting parameters of X-ray lines with substructure features of material, GPF of coherent block size D , lattice distortion ε , dislocation density ρ and lattice elastic deformation $\Delta d/d_{av}$ can be constructed, so that, instead of some single rather accidental value, the substructure condition is characterized by the spectrum of values, corresponding to local conditions in grains with different orientations and different volume fractions.

Values ε and $\Delta d/d_{av}$ characterize elastic deformation of the crystalline lattice at different scale levels — at the microlevel of grains with the definite orientation and at the mesolevel of grain groups, representing the texture of material, respectively. Calculation of ε bases on the presentation of an X-ray line profile as the superposition of mutually shifted X-ray lines by assumption, that reflecting grains contain fragments, differing in interplanar spacing due to local elastic deformation. By calculation of $\Delta d/d_{av}$ it is assumed, that grains of each orientation are characterized by the measured most probable interplanar spacing, while d_{av} indicates the level, average for grains of all orientations.

3. Principles of substructure inhomogeneity

Authors employed the GPF method in studies of numerous metal materials, deformed by rolling. As a typical example, in Fig.2 PF{011} (a), GPF $\beta_{022}(\alpha, \varphi)$ (b) and GPF $2\theta_{022}(\alpha, \varphi)$ (c) are presented for the β -Zr phase in rolled quenched alloy

Zr-20%Nb. Hatching shows zones of increased values of the pole density in PF{011} (a), the physical half-width in GPF β_{022} (b) and the Bragg angle in GPF $2\theta_{022}$ (c).

Consideration of all obtained GPF testifies that the structure of deformed metal includes an extremely wide spectrum of substructure conditions. Within GPF for rolled metal materials the true half-width β of X-ray lines by intermediate Bragg angles varies usually from $0.2^\circ \div 0.6^\circ$ up to $2.0^\circ \div 2.5^\circ$, that covers the whole interval of practically observable values. The lower boundary of this interval is quite distinct always and corresponds to rather coarse coherent blocks (50–60 nm) by insignificant lattice distortions (10^{-6}). However, its upper boundary, corresponding to the extreme fragmentation of coherent blocks and highest lattice distortions, is beyond reach for detection, since usually the wider is the X-ray line the lower are both its maximal intensity and the measurement accuracy. Usual range of the peak position 2θ in the corresponding GPF of textured metal materials shows, that the actual elastic deformation of the crystalline lattice locally proves to be essentially higher than its conventional limit of 0.2%.

Hence, in the same sample the substructure condition of crystallites varies within a very wide range: side by side with large blocks, having the relatively perfect lattice, there is a fraction, characterized by extremely small coherent domains and/or the utmost lattice distortion.

When comparing positions of maxima and minima in GPF of integral intensity and line broadening, it becomes evident that minima of line broadening coincide with texture maxima, whereas maxima of line broadening are localized within texture minima (see Fig.2-a,b). Let the totality of substructure factors, responsible for an increase of the physical line broadening, be designated by the term "residual deformation effects".

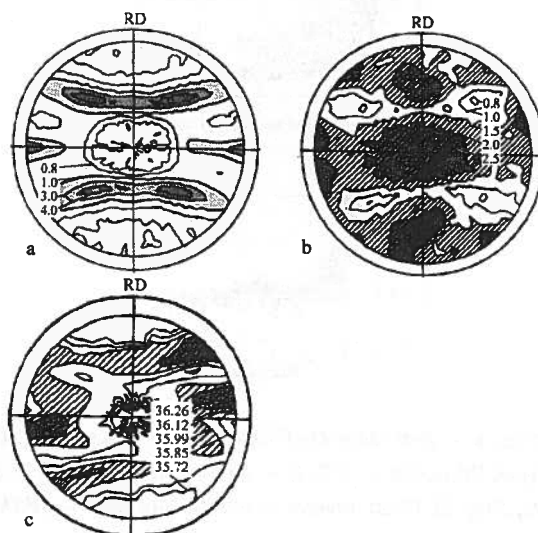


Fig. 2. Substructure inhomogeneity of β -Zr in the rolled quenched Zr-20%Nb alloy: a — PF {011}; b — GPF β_{022} (in deg.); c — GPF θ_{022} (in deg.). Angular radius — 70°

Then it can be stated, that residual deformation effects are minimal in texture maxima and increase up to highest values by passing to texture minima. This is the most general rule, controlling the substructure inhomogeneity of textured materials.

The dependence of the substructure condition on the place of crystallites in the texture of material is analyzed by diagrams of correlation between GPF β_{hkl} and GPF I_{hkl} or PF(hkl). In order to construct such a diagram, values of β_{hkl} and I_{hkl} are determined for each orientation (ψ, φ) of reflecting planes (hkl), that is for each point (ψ, φ) in both GPF, and then they are used as ordinates and abscissas of points in the correlation diagram. In Fig.3 correlation diagrams are presented for: (a) β -Zr of rolled quenched alloy Zr- 20%Nb; (b) the cold-rolled Nb foil; (c) α -Zr of Zr-1%Nb alloy.

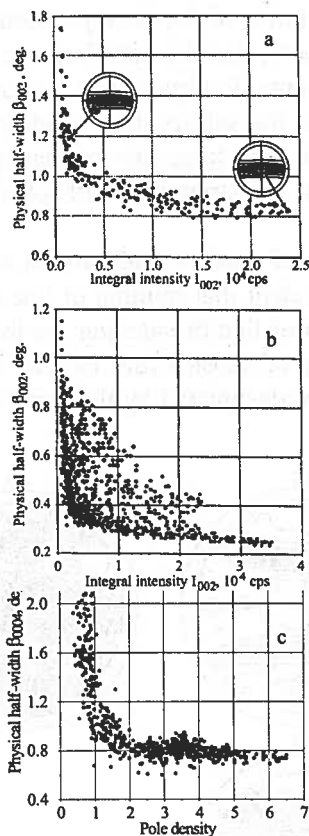


Fig. 3. Correlation diagrams: a — β -zr alloy Zr-20%Nb, eolling + quenching, GPR β_{002} — GPF I_{002} ; angular radius of embraced PF region — 25° ; b — cold-rolled Nb foil, GPF β_{002} — GPF I_{002} ; PF radius — 70° ; c — α -Zr, alloy Zr-1%nb, transverse rolling, Gpf β_{004} — PF(0001), PF radius — 60°

Both β -Zr (a) and Nb (b) have the BCC crystalline lattice and rolling textures with the same main component $\{001\} \langle 011 \rangle$, but their diagrams cover regions of PF with different radii — 25° and 70° , respectively. Whereas (a) covers only the

central part of PF{001}, including the single texture maximum of the component $\{001\}\langle 011\rangle$ and its vicinity, (b) includes, along with the component $\{001\}\langle 011\rangle$, the zone of the component $\{011\}\langle 001\rangle$ at a distance of 40° – 50° from the center [6]. Both diagrams have a typical descending character, connected with the component $\{001\}\langle 011\rangle$, but the diagram for Nb contains in its inner part the additional descending branch, corresponding to the component $\{011\}\langle 001\rangle$, characterized by the higher strain hardening.

The diagram for α -Zr (Fig.3-c) shows, that the found principle of substructure inhomogeneity is true for the phase with HCP crystalline lattice as well. The used alloy Zr- 1%Nb was submitted to transverse rolling up to formation of the intermediate quasi-stable texture with main components $(00.1)\pm 15\div 20^\circ\text{ND-RD}\langle 11.L\rangle$ [8], so that, unlike the case of the final rolling texture, basal axes of all its crystallites are localized in the central part of PF(0001) and acting mechanisms of their plastic deformation are more or less similar.

A regular character of the diagram confirms the above rule and gives a basis for its quantitative interpretation. By passing from texture maxima to texture minima the true half-width of X-ray line gradually increases, showing different characters of this tendency for texture maxima and texture minima: a slow growth of the line broadening within texture maxima gives place to its sharp increase within texture minima, while statistical significances of data for both regions are equally high.

Besides differences in substructure of regions, corresponding to texture maxima and minima, there are systematic substructure differences between crystallites of main texture components. This can be illustrated, in particular, by example of the same Nb foil. Its rolling texture contains two groups of main components: $\{001\}\langle 112\rangle\langle 011\rangle$ and $\{011\}\langle 001\rangle$. Their arising is conditioned by operation of different deformation mechanisms, resulting in different levels of strain hardening. Points of PF{001}, belonging to the components $\{001\}\langle 112\rangle\langle 011\rangle$ and adjacent minima, form in the correlation diagram (Fig.3-b) the sharp lower contour of the distribution, whereas points from vicinity of the component $\{011\}\langle 001\rangle$ form an additional upper branch of the distribution. The latter is less distinct, since the corresponding area of PF contains comparatively small number of points. An analysis shows that the strain hardening of crystallites, belonging to main stable components of the deformation texture, increases with lowering of the Schmid factor in acting slip systems [9].

The same rule of substructure inhomogeneity is valid not only for deformed polycrystalline materials, but also for rolled single crystals. An extensive cycle of experiments on rolling of single crystals from Ti-48%Ni-2%Fe alloy in B2-phase with BCC crystalline lattice by 11 initial orientations was realized [10]. Obtained rolled samples show a variety of deformation textures depending on the initial orientation and the deformation degree — from simplest ones, consisting of the single component, to multi-component textures, similar to those in rolled polycrystals. The development of substructure inhomogeneity and microstrain distribution in rolled single crystals by gradual complications of their texture were studied systematically by the GPF method.

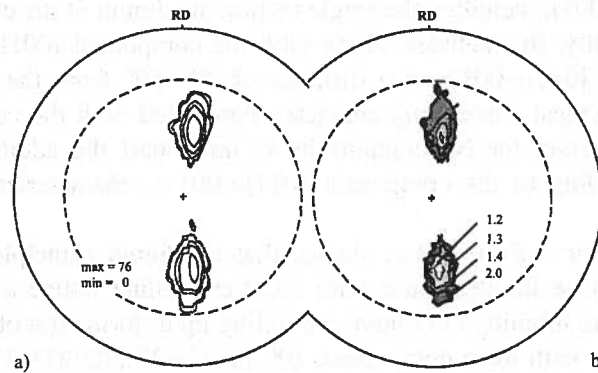


Fig. 4. Substructure inhomogeneity of the rolled Ti-Ni single crystal with the stable initial orientation $\{011\}\langle 110\rangle$, $\varepsilon = 77\%$: (a) PF $\{001\}$, (b) GPF β_{002} (in deg.)

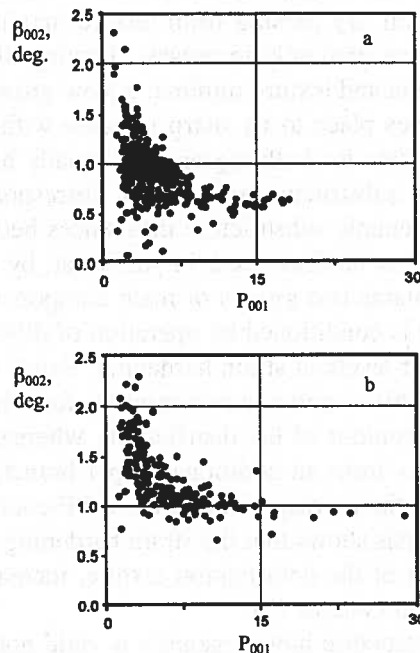


Fig. 5. Diagrams of correlation between PF $\{001\}$ and GPF β_{002} for Ti-Ni single crystals, rolled in the initial orientation $\{001\}\langle 001\rangle$ up to $\varepsilon_1 = 15\%$ (a) and $\varepsilon_2 = 44\%$ (b)

In Fig.4 PF $\{001\}$ and GPF β_{002} are presented for the Ti-Ni single crystal, rolled in the stable orientation $\{011\}\langle 011\rangle$ up to deformation degree 77%. As a result of rolling, within relatively narrow texture maxima the distribution of X-ray line half-width developed, characterized by the same features, as shown above for rolled polycrystalline materials: in the center of the texture maximum β_{002} is minimal ($< 1.0^\circ$) and grows

to the periphery up to 2.0° . Correlation diagrams in Fig.5 demonstrate formation of the regular substructure inhomogeneity in the Ti-Ni single crystal, rolled in the initial orientation $\{001\}\langle 001\rangle$: by passing from $\varepsilon_1 = 15\%$ (a) to $\varepsilon_2 = 44\%$ (b) the X-ray line half-width β_{002} for most fragments of the rolled single crystal increases and its correlation with pole density becomes more distinct. Thus, in rolled single crystals the same type of substructure inhomogeneity develops as in polycrystals, though in considered cases its separate fragments had very close trajectories in the orientation space.

Hence, there are two factors, controlling the condition of crystalline lattice along the normal to reflecting planes. The first factor is belonging of grains to that or another texture component, connected with different biographies of corresponding crystallites, including different initial orientations and different trajectories in the orientation space. The second factor is the position of crystallite in the center of texture maximum or at its periphery, closer to texture minimum. Besides, there is the third factor, influencing the lattice condition along axes of the interest — the substructure anisotropy within each grain. This factor is considered in the last section of the paper in more details.

Physical reasons for the first and the third factors are rather evident, whereas the second factor, that is belonging of the grain to texture maximum or texture minimum, needs some explanation. The most evident explanation is the following. The texture development accompanies the plastic deformation by crystallographic mechanisms. By sufficiently high deformation degrees the central part of texture maximum corresponds to the stable orientation of grains under the used loading. The symmetric stable orientation is maintained by simultaneous operation of several mutually balanced slip systems. When distortion of the crystalline lattice within some fragment proves to be too high because of too high content of defects, balanced operation of several slip systems within this fragment becomes impossible and its orientation shifts from the symmetric stable position. Therefore at the periphery of texture maxima and in texture minima there are fragmented grains with the most distorted crystalline lattice, whereas grains with the relatively perfect lattice remain at the center of texture maximum and retain the symmetric stable position. Finest fragments of grains with the too distorted crystalline lattice lose the ability to deform by means of crystallographic mechanisms, so that their final orientations prove to be occasional; texture minima contain only such grains. Hence, a position of the grain relative to texture maxima and minima depends on its ability to maintain the correct action of crystallographic deformation mechanisms. Evidently, this ability becomes lower with an increase of the dispersity of coherent blocks and the lattice distortion.

There is one more factor, influencing the lattice condition along axes of the interest — the substructure anisotropy within each grain, consisting in different substructure conditions along crystallographic axes of the same type, correlating with the anisotropy of loading by deformation. In principle, GPF β_{hkl} describes the lattice condition along axes $\langle hkl \rangle$ irrespective of their belonging to grains of that or another orientation, and in order to reveal the substructure anisotropy in grains with some concrete orientation, one ought to construct ODF and to bring it into correlation with GPF β_{hkl} . This paper

does not deal with such a procedure, though it is realizable on the basis of acceptable data.

4. Distribution of residual elastic microstrains

Since elastic microstresses, or residual stresses of 2-nd kind, by definition are equilibrated within several neighbouring grains [11], the volume irradiated by texture diffractometric measurements usually is sufficiently large to satisfy conditions for this equilibrium. Hence, measured GPF 2θ are formed by X-ray reflections from grains (subgrains, domains and the like), whose crystalline lattice experiences alternatively elastic deformations of opposite signs relative to the average level, determined by elastic macrostresses. This assertion is confirmed by the diagram of correlation between GPF I_{002} and GPF $2\theta_{002}$ for the rolled Nb foil in Fig.6 [6]. Its approximate symmetry about the central line testifies, that each point (ψ, φ) of PF{001} has its pair $(\psi, \varphi)^*$, characterized by the same integral intensity I_{002} and by the elastic deformation $\Delta d/d_{av}$ of the same absolute value with the opposite sign.

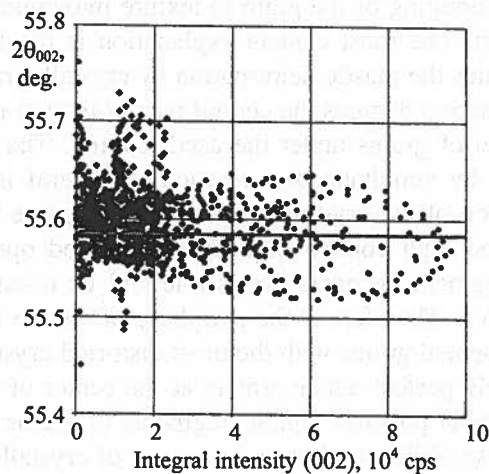


Fig. 6. Diagram of correlation between PF{001} and GPF $2\theta_{002}$ for the Nb foil

The total equilibrium of residual microstresses realizes in the studied sample in connection with the observed distribution of elastic deformation. In the general case of polycrystalline material with a rolling texture, tensile and compressive microstresses prove to be mutually equilibrated about PF diameters, corresponding to symmetry planes of the deformation scheme by rolling. The distribution of the Bragg angle $2\theta_{022}$ in Fig.2-c distinctly manifests, that cross-hatched zones of increased 2θ values are shifted relative to the texture maxima to their slopes and that the distributions within first and third as well as second and fourth quadrants are rather similar. The analogous mode of microstress equilibrium takes place in many polycrystalline materials with

developed rolling textures. When considering GPF $(\Delta d/d_{av})_{hkl}$ for high symmetry axes $\langle hkl \rangle$, quadrants with predominant extension and compression of the crystalline lattice along these axes alternate in the stereographic projection of the rolled sample, so that residual elastic microstresses prove to be equilibrated about symmetry planes of the loading scheme.

The most distinct illustration of such equilibrium is seen in GPF $\Delta d/d_{av}$ for HCP metal phases with developed rolling textures. For example, in Fig.7 PF(0001) and GPF $\Delta c/c_{av}$ are presented for the ω -Zr phase in the rolled alloy Zr-20%Nb [12]. In this case elastic microstrains are distributed in such a manner, that zones of extension and compression are aligned parallel with texture maxima at their opposite slopes and form the cross-wise pattern, whereas main diameters of PF separate these zones with opposite signs of residual elastic deformation.

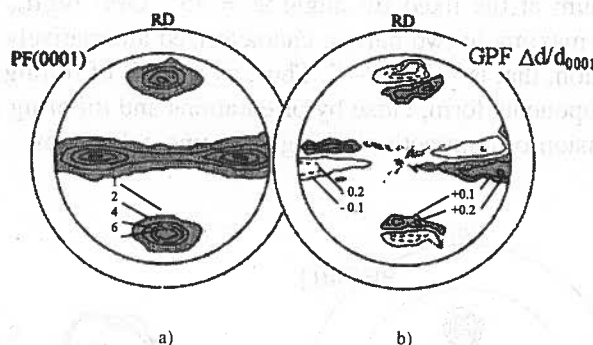


Fig. 7. The distribution of lattice elastic microstrains along axes $\langle 0001 \rangle$ in the ω -phase of the quenched rolled alloy Zr- 20%Nb: (a) PF(0001), (b) GPF $\Delta c/c_{av}$

It should be noted, that a precision of X-ray experimental evidences, confirming the regular symmetric character of residual microstress distributions, is inevitably restricted by a number of factors, among which there are the following: insufficient statistics, incomplete pole figures, non-ideal geometry of the rolling scheme, surface effects, some fraction of low-quality measurements by high values of the tilt angle ψ . Nevertheless, the pairwise similarity of odd and even quadrants in GPF 2θ (Fig. 2-c), GPF $\Delta c/c_{av}$ (Fig. 7) as well as the symmetry of correlation diagram in Fig. 6 are quite evident, though can be stated only to some approximation. As for the principle of microstress equilibrium, following from these experimental results, it covers axes $\langle 001 \rangle$ or $\langle 011 \rangle$ of all crystallites within the studied volume $10 \text{ mm} \times 1 \text{ mm} \times 0.01 \text{ mm}$ and can not be considered as based on some accidental data collection. This actual mode of microstress equilibrium is an experimental fact and could not be foreseen on the basis of speculative simulation.

Thus, GPF $2\theta_{hkl}$ reveals an anisotropy of elastic deformation of grains $d_{hkl}(\psi, \varphi)/d_{av}$ along axes $\langle hkl \rangle$ due to action of residual microstresses. The main result, which becomes evident by consideration of GPF $2\theta_{hkl}$ (or GPF $\Delta d_{hkl}/d_{av}$) for deformed materials, is the following: the interplanar spacing d_{hkl} changes continuously, when passing

from of $PF\{hkl\}$ to another, differing in the orientation of reflecting planes. Hence, the concept of interplanar spacing — especially, as applied to deformed samples — has a sense only on condition that it is determined as a distribution.

Moreover, a significant inhomogeneity of d_{hkl} distribution takes place not only in deformed polycrystals, but even in rolled single crystals with the sharp one-component texture. Fig.8 illustrates this situation for the Ti-Ni single crystal, rolled by $\epsilon = 10\%$ in the stable initial orientation $\{011\}\langle 011 \rangle / 10/$. After rolling the single crystal retains its orientation (Fig.8-a), showing only insignificant additional scattering without formation of high-angle boundaries. Profiles of the X-ray line (002), registered in successive numerated points within the texture maximum of Fig.8-b, are presented in Fig.8-d. A vertical line marks the weighted average value of the Bragg angle, calculated for the whole PF. The gradual shift of the peak position is observed as we go through the texture maximum at the fixed tilt angle $\psi = 45^\circ$. GPF $\Delta d/d_{av}$ in Fig.8-c shows division of texture maxima in two halves, characterized alternatively by opposite signs of elastic deformation, that is “+” or “-”. Thus, as a result of rolling, within the single crystal two subcomponents form, close by orientations and differing in types of elastic deformation (extension or contraction) along the same cubic axes.

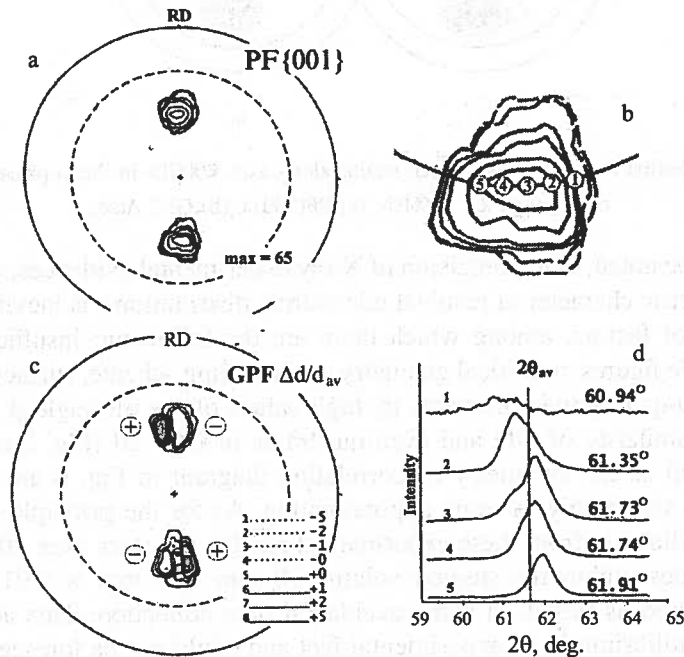


Fig. 8. Distribution of microstrains in the Ti-Ni single crystal, rolled by $\epsilon = 10\%$ in orientation $\{011\}\langle 011 \rangle$: a — $PF\{001\}$, angular radius — 70° ; b — the lower texture maximum of (a) with reference points; c — $GPF \Delta d_{001}/d_{av}$ ($\% \times 10^2$); d — profiles of X-ray line (002), corresponding to successive points in (b)

The possibility to determine tensors of residual strain and stress for separate grains of the polycrystal using the GPF method is evident by the example of the Ti-Ni single crystal, rolled by $\varepsilon = 58\%$ in the initial orientation $\{001\}\langle 011 \rangle$. Its rolling texture consists of two equivalent components $\sim\{111\}\langle 011 \rangle$, denoted as A and B. Crystallites of B2-phase have three axes $\langle 001 \rangle$ each, so that in PF $\{001\}$ both components have three texture maxima each, marked in PF with different badges depending on their position (Fig.9-a). The same badges are used in diagrams of correlation between GPF I_{002} and GPF $2\theta_{002}$ in Fig.9-b,c for components A and B, respectively. While the upper texture maximum of A-component manifests the increase of d_{001} and its lower maximum — the decrease of d_{001} (Fig.9-b) with respect to the average level, texture maxima of B-component exhibit the reverse trend (Fig.9-c). At the same time, the interplanar spacing d_{001} along axes $\langle 001 \rangle$, having their projections within central texture maxima of both components, shows minimal deflections from the average level by elastic deformation of the lattice. In this case the equilibrium of microstresses realizes due to elastic interaction of crystallites, belonging to components with opposite types of strain anisotropy.

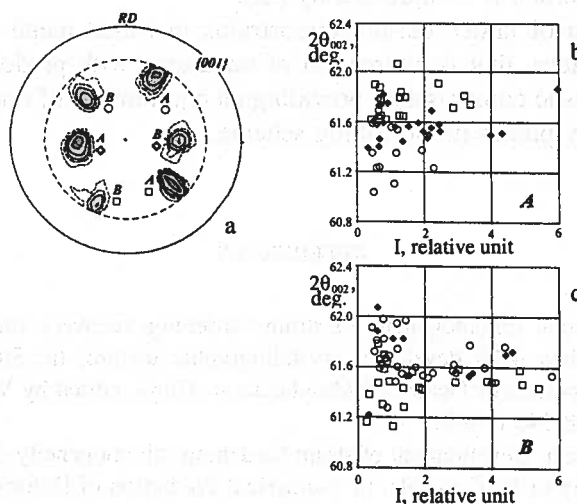


Fig. 9. Anisotropy of residual elastic microstrains in rolled by $\varepsilon = 58\%$ Ti-Ni single crystal: a — PF $\{001\}$; b,c — diagrams of correlation I_{002} – $2\theta_{002}$ for texture maxima of components A (b) and B (c)

As for the revealed mode of residual microstress equilibrium in deformed metal materials, it could not be predicted on the basis of some speculative model. The most general idea concerning the concrete realization of microstress equilibrium comes to the primitive supposition, that this equilibrium is attained due to opposite elastic deformation of neighbouring grains. However, according to above experimental results, obtained by the GPF method, a regular system in microstress distribution proves to be evident only in the orientation space, that is by systematization of this distribution on the basis of criterion, connected with grain orientations.

5. Conclusions

1. The structure of deformed metal includes an extremely wide spectrum of substructure conditions, implying lattice distortion, coherent domain size, dislocation density etc..
2. The grain orientation is the most effective criterion for systematization of substructure inhomogeneities in textured materials.
3. Grains of main texture components differ in their substructure conditions due to different "biographies" and acting deformation mechanisms.
4. Residual deformation effects are minimal in texture maxima and gradually increase up to the highest level by passing to texture minima, since the grain position relative to texture maxima and minima is determined by its capability to maintain the balanced operation of several mutually symmetric slip systems.
5. The equilibrium of elastic microstresses in textured metal materials realizes in such a manner, that for each grain with the crystalline lattice, extended along axis $\langle hkl \rangle$ by $(+\varepsilon)$, there is its pair with the symmetric orientation, where along axis $\langle hkl \rangle$ the crystalline lattice is compressed by $(-\varepsilon)$.
6. The distribution of lattice elastic microstrains in rolled metal materials shows a cross-wise pattern, that is alternation of quadrants with predominance of elastic extension or elastic compression, providing an equilibrium of microstresses relative to the symmetry planes in the rolling scheme.

REFERENCES

- [1] Yu. Perlovich, Inhomogeneity of strain hardening, recovery and recrystallization in molybdenum alloys with developed crystallographic texture. In: Structure, Texture and Mechanical Properties of Deformed Molybdenum Alloys, edited by V.I. Trefilov, Naukova Dumka, Kiev, 88-145 (1983).
- [2] Yu. Perlovich, Development of strain hardening inhomogeneity during texture formation under rolling of BCC-metals. In: Numerical Prediction of Deformation Processes and the Behaviour of Real Materials, Proceedings of 15th Riso International Symposium on Materials Science. Eds. S.I. Andersen et al.. Riso National Laboratory, Roskilde, Denmark 445-450 (1994).
- [3] Yu. Perlovich, Inhomogeneous recrystallization in rolled textured CC- metals. In: Microstructural and Crystallographic Aspects of Recrystallization, Proceedings of 16th Riso International Symposium on Materials Science. Eds. N. Hansen et al.. Riso National Laboratory, Roskilde, Denmark, 485-490 (1995).
- [4] Yu. Perlovich, Text. & Microstr. **25**, 129-147 (1996).
- [5] Yu. Perlovich, H.J. Bunge, M. Isaenkova, Text. & Microstr. **29**, 241-266 (1997).
- [6] Yu. Perlovich, H.J. Bunge, M. Isaenkova, Z. Metallkd. **91**, 149-159 (2000).
- [7] B.E. Warren, X-ray Diffraction, Addison-Wesley Publishing Company, Massachusetts (1969).

- [8] G. Wassermann, J. Greven., Texturen metallischer Werkstoffe, Springer-Verlag, Berlin — Gottingen — Heidelberg (1962).
- [9] M. Isaenkova, Yu. Perlovich, Proceedings of the USSR Academy of Science. Metals 3, 152-155 (1987).
- [10] Yu. Perlovich, H.J. Bunge, M. Isaenkova, V. Fesenko, R. Rustamov, Text. & Microstr., 31, 53-84 (1998).
- [11] A. Taylor, X-ray Metallography, John Wiley & Sons, Inc., New York - - London (1961).
- [12] Yu. Perlovich, H.J. Bunge, M. Isaenkova, V. Fesenko, Text. & Microstr. 33, 303-319 (1999).

Received: 21 March 2005.